Pd polarization and interfacial moments in Pd-Fe multilayers

L. Cheng, Z. Altounian, D. H. Ryan, J. O. Ström-Olsen, and M. Sutton
Physics Department and Centre for the Physics of Materials, McGill University, 3600 University Street, Montreal, Quebec, Canada H3A 2T8

Z. Tun
Neutron Programme for Materials Research, Steacie Institute for Molecular Sciences, National Research Council, Chalk River Laboratories, Ontario, Canada K0J 1J0

(Received 21 January 2004; published 2 April 2004)

A combination of bulk magnetization, conversion electron Mössbauer spectroscopy, and polarized neutron reflectometry is used to show that in Pd/Fe multilayers at 4.5 K there is a slight ($\sim$10%) enhancement of the Fe moment at the Pd/Fe interface, and that the Pd is almost maximally polarized, with an average moment of $0.32\mu_B$ to a depth of about 20 Å from the Pd/Fe interface. The Pd polarization is strongly temperature dependent.

DOI: 10.1103/PhysRevB.69.144403 PACS number(s): 75.70.−i, 61.12.Ha, 71.70.Ch, 76.80.+y

I. INTRODUCTION

Bulk palladium metal is a strongly enhanced paramagnet[1] that requires as little as 0.1 at. % of a $3d$ impurity (Mn, Fe, Co, Ni) to induce ferromagnetism.[2–5] The magnetization in these dilute alloys is too large to be due to the impurity alone[6,7] suggesting that the solute atom polarizes the surrounding Pd atoms to form a ''giant'' moment. In very dilute alloys, where the overlap between giant moments is minimal, the total moment of a polarized cloud may be as much as $\sim 10\mu_B$,[2,8,9] with average Pd moments of $0.05\mu_B$–$0.4\mu_B$.[2,10,11] The spatial extent of the polarization cloud is not well known. Ascribing the onset of long-range ferromagnetic order to the formation of a percolating network of giant moments implies a radius of $\sim$30 Å.[4] Alternatively, with Pd carrying $(0.1–0.3)\mu_B$/atom (values taken from concentrated Pd-Fe alloys[12,13]), a uniform, maximally polarized cloud would have to extend 5–10 Å from the central impurity to account for the observed $\sim 10\mu_B$ cloud moment. Finally, direct determination using small-angle neutron scattering yields values ranging from 10 Å (Refs. 11,14, and 15) to 50 Å.[16] While these scattering-based estimates of the cloud's extent have been questioned,[17] band-structure calculations confirm that many hundreds of Pd atoms should be polarized.[18]

The wide range of estimates for both the size and amplitude of the polarization cloud reflects experimental difficulties associated with extremely dilute random alloys. The small-angle scattering signal is weak, and necessarily contains contributions from many dynamic and static disorder sources. The problem can be greatly simplified by studying Pd-Fe multilayers, where the system can be regarded as almost one dimensional, and the materials involved are pure metals. Furthermore, the magnetic behavior will be simpler as the Pd is in contact with bulk-like, ferromagnetically ordered iron layers rather than isolated, randomly ordered Fe impurity atoms. While many thin-film and multilayer Pd-Fe studies exist, no consensus on either the iron moment at the Pd/Fe interface or the extent and magnitude of the magnetic polarization in the Pd layers has emerged.

We have therefore undertaken a series of complementary measurements on a single system. The work presented here has the following important features: We combine bulk magnetic characterization for total moments with microscopic data from conversion electron Mössbauer spectroscopy (CEMS) so that we can distinguish the Fe and Pd contributions to the observed temperature dependences of the bulk magnetization; we then use polarized neutron reflectometry (PNR) to probe the magnitude and depth of the induced polarization in the Pd layers, using multilayer samples grown with carefully matched Pd and Fe layer thicknesses in order to minimize the chemical structure contributions to the even-order superlattice reflections[19] so greatly enhancing sensitivity to Pd polarization effects. Taken in isolation, no single measurement can yield an unequivocal understanding of Pd/Fe layer moments; taken together, a clear conclusion emerges.

We find (i) that there is a clear excess magnetization associated with polarization of the Pd layers; (ii) that the excess is strongly temperature dependent and falls an order of magnitude faster than the magnetization of the Fe layers; (iii) that the Fe moment at the Pd/Fe interface is enhanced; and (iv) that the Pd is polarized to about $0.32(2)\mu_B$/Pd to a depth of 20(4) Å at 4.5 K.

II. PREPARATION AND STRUCTURAL CHARACTERIZATION

The multilayers were deposited using dc magnetron sputtering at ambient temperature onto Si substrates with their native oxide surface. The base pressure prior to sputtering was 2.0×10^{-7} Torr, and the Ar pressure during sputtering was 7 mTorr. 99.99% Fe and 99.9% Pd targets were used. The deposition rates, monitored by quartz-crystal sensors and calibrated using x-ray reflectometry measurements, were about 1 Å/s and 2 Å/s for Fe and Pd, respectively. Two groups of multilayers were prepared. The first group ($[\mathrm{Pd}\ 50\ \text{Å}/\mathrm{Fe}\ t\ \text{Å}]_{25}$) (nominal $t = 5, 10, 15, \ldots, 40$ Å) was deposited on 0.5 mm thick, 20 mm diameter Si(100) substrates and used for magnetometry, CEMS and initial PNR

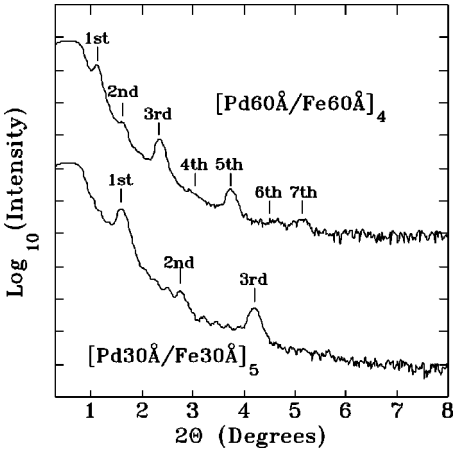

FIG. 1. x-ray reflectivity curves for the two layer matched Pd-Fe multilayer samples prepared for PNR. Note the greatly reduced signals at the even-order positions.

work, while the second set, for PNR ($[\mathrm{Pd60\ \AA/Fe60\ \AA}]_4$ and $[\mathrm{Pd30\ \AA/Fe30\ \AA}]_5$), was deposited on 6.35 mm thick, 100 mm diameter Si(111) substrates. The larger area was to increase the scattered signal while the thicker substrate provided better mechanical stability. Matching between the Pd and Fe thicknesses was confirmed by x-ray reflectometry.

High-angle Cu$K\alpha$ x-ray-diffraction patterns showed that all of our Pd/Fe multilayers exhibited preferential Pd(111)/Fe(110) orientation. The appropriate d spacings ($d_{\mathrm{Pd(111)}} = 2.2464$ Å, $d_{\mathrm{Fe(110)}} = 2.0269$ Å) were therefore used to convert the layer thicknesses from angstrom to atomic layers (AL) for the analysis of the magnetic data. Low-angle x-ray reflectometry measurements were used to determine the layer thicknesses and to establish the sample quality.

Low-angle Cu$K\alpha$ x-ray measurements were carried out on a high-resolution triple-axis four-circle diffractometer. Superlattice peaks for both series were seen to sixth order without significant broadening, indicating a well-defined compositional modulation along the film growth direction. The bilayer thicknesses for the first series were determined by fitting reflectivity profiles, yielding a constant Pd thickness of 53(1) Å, with the Fe layer thickness increasing in steps of 4.8(2) Å. The actual Fe and Pd thicknesses for the second series samples used in the PNR study are 61 and 34 Å, respectively. Figure 1 clearly shows that careful matching of the Pd and Fe layer thicknesses in the second series of samples leads to a substantial suppression of the even-order reflections.[19] This reduced chemical structure contribution at the even-order positions in layer-matched samples leads to a greatly enhanced sensitivity in the PNR data to magnetic polarization of the Pd by the Fe moments.

At 34 Å the Pd layer in the thinner of the two PNR samples was found to be fully polarized, so no direct information on the Pd moment could be obtained from this sample. The results were found to be fully consistent with those from the 61 Å sample, but they will not be discussed further here.

III. MAGNETIC CHARACTERIZATION

^{57}Fe CEMS spectra were collected using a He+10% CH_4 gas-flow proportional counter installed in a nitrogen-flow cryostat operated down to 90 K (Fig. 2). The CEMS results have been published elsewhere[20] and so will only be summarized here. Two Fe contributions can be distinguished; one from the bulk, the other associated with the Pd/Fe interfaces. The total interfacial Fe thickness was estimated from the relative areas of the two contributions and is 8(1) Å per Fe layer. Assuming that this is distributed equally on each side of the Fe layers, then ~4 Å [or 2.0(3) AL] of Fe are interfacelike at each Pd/Fe interface.

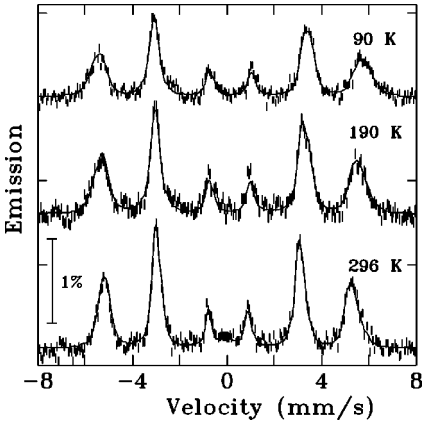

FIG. 2. Conversion electron Mössbauer spectra for the $[\mathrm{Pd\ 24\ AL/Fe\ 7.2\ AL}]_{25}$ multilayer at various temperatures showing clear in-plane magnetic texture at all temperatures (lines 2 and 5 are much stronger than 1 and 6) and a gradual increase in hyperfine field on cooling.

Inspection of the CEMS spectra in Fig. 2 shows that the outer lines broaden on cooling. This reflects the slightly stronger temperature dependence of the hyperfine field B_{hf} in the more widely split Pd/Fe interfacial component. Analysis of the temperature dependence of B_{hf} for the two components (Fig. 3) shows that the hyperfine field of the interfacial component is larger than that of the bulk, and if we assume a simple linear scaling between B_{hf} and μ_{Fe}, then this translates into a slightly enhanced moment of $2.38(2)\mu_B$/Fe at

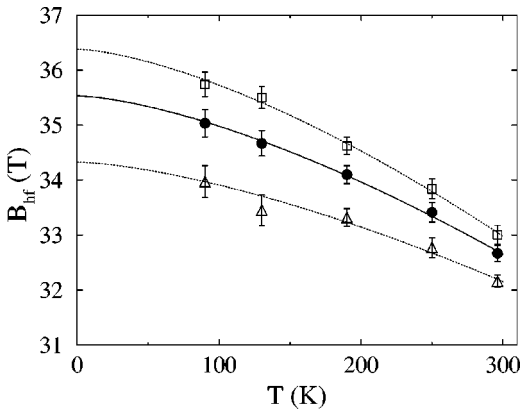

FIG. 3. Temperature dependence of the hyperfine field B_{hf} of the bulk (△) and Pd/Fe interface (□) components for the $[\mathrm{Pd\ 24\ AL/Fe\ 7.2\ AL}]_{25}$ multilayer sample. Also shown is the area-weighted average B_{hf} (●). The lines are $T^{3/2}$ fits used to extend the data to lower temperatures for comparison with the magnetization data.

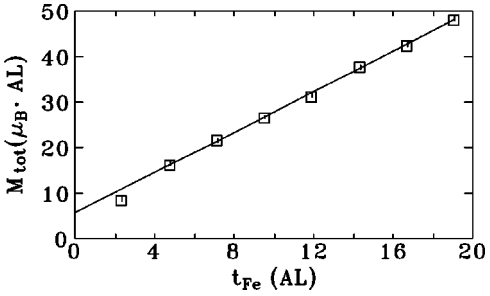

FIG. 4. M_{tot} vs Fe thickness at 5 K for $[\text{Pd 24 AL/Fe } t \text{ AL}]_{25}$ multilayers with $t=2.4$–19.1 AL. Solid line is a fit to Eq. (1) (see text).

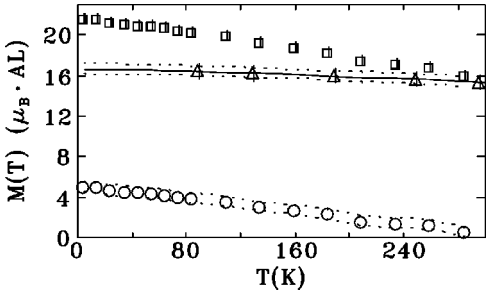

FIG. 5. The temperature dependence of the palladium polarization M'_{Pd} (○) obtained by subtracting M_{Fe} (△—derived from CEMS data) from M_{tot} (□) for $[\text{Pd 24 AL/Fe 7.2 AL}]_{25}$ (see text). Dotted lines indicate the range of uncertainty in M_{Fe} and M'_{Pd} arising from uncertainties in the thickness of the interfacial Fe component and its moment. Solid line through CEMS data is $T^{3/2}$ fit used to extend the data down to 5 K.

the Pd/Fe interfaces. Our interfacial layer thickness is consistent with earlier CEMS work,[21] however both reduced[22] and enhanced[23] interfacial hyperfine fields have been reported. As shown below, PNR confirms the presence of an enhanced interfacial Fe moment.

Magnetization measurements were made using a Quantum Design PPMS operated between 5 K and 290 K in fields of up to 3 T. The linear dependence of the total magnetization (M_{tot}) on the Fe layer thickness (t_{Fe}) shown in Fig. 4 suggests that (except for the thinnest Fe layer) the bulk (m_b) and interfacial (m_i) Fe moments and the Pd polarization (M_{Pd}) are independent of t_{Fe}, so that we can write

$$M_{tot}=m_i\times 2t_i+m_b\times(t_{Fe}-2t_i)+M'_{Pd}, \qquad (1)$$

where t_i is the thickness of one interfacial Fe layer and $M'_{Pd}=M_{Pd}(\sigma_{Pd}/\sigma_{Fe})$, where σ_{Pd} and σ_{Fe} are the in-plane densities of Pd(111) and Fe(110), respectively. The departure from linearity below $t_{Fe}=4.8$ AL indicates that $2t_i \leqslant 4.8$ AL, consistent with our CEMS value of $2t_i = 4.0(6)$ AL. The slope of the line in Fig. 4 is $m_b = 2.22(3)\mu_B$, consistent with bulk Fe. The intercept, which corresponds to $M'_{Pd}+(m_i-m_b)2t_i$ is $5.7(4)\mu_B\times$AL. Taking $m_i=2.38(2)\mu_B$/Fe and $t_i=2.0(3)$ AL from our CEMS data, we find that the interfacial Fe contribution to this intercept is $\sim 0.6(2)\mu_B$, just over 10% of the total, implying that there must be significant polarization of the Pd. Taking the average Pd moment as $0.3\mu_B$ (from our PNR data below) implies that the total polarized layer is 19(2) AL or 43(4) Å thick (half being on each side of the Fe layer). Furthermore, using the temperature dependence of the hyperfine fields[20] we can extend the CEMS data below 90 K (the total extrapolated change in this region is less than 3%), and so estimate the contributions of the bulk and interfacial Fe to the magnetization. Subtraction from the measured total then yields an estimate of the temperature-dependent Pd polarization (Fig. 5). Note that almost no polarization survives in the palladium layers at room temperature. This feature will be exploited in the analysis of the PNR data.

IV. POLARIZED NEUTRON REFLECTOMETRY

PNR measurements were carried out on the C5 spectrometer of the DUALSPEC facility at the Chalk River Laboratory. Neutrons with a wavelength of 2.37 Å were Bragg reflected from a Heusler alloy (Cu_2MnAl) monochromator, and spin analyzed by another Heusler crystal after being reflected by the sample. Mazei flippers located before and after the sample enabled the measurement of all four spin-dependent scattering channels: non-spin-flip (NSF) (R^{++} and R^{--}) and spin-flip (SF) (R^{+-} and R^{-+}). An in-plane magnetic field of 25 mT provided by permanent magnets saturated the multilayers as verified by extremely low SF scattering. Hence, only NSF channels were measured subsequently over the Q range 0.004–0.35 Å^{-1}. Reflectivities measured at ambient (RT) and 4.5 K are shown for the $[\text{Pd 60 Å/Fe 60 Å}]_4$ sample in Fig. 6.

As neutrons interact with both the nuclei and the atomic moments, both chemical and magnetic structures contribute to the observed NSF scattering. Moreover, the two scatterings occur at the same Q for a ferromagnet, since there is no development of new periodicity. This generally makes the detection of additional magnetic moments difficult in ferromagnets. In our case, the magnetic contribution can be manipulated in three ways: (i) the Pd polarization is expected to be more strongly temperature dependent than the Fe magnetization (Fig. 5); (ii) in appropriate units the R^{++} channel is the (Fourier transform) (Ref. 2) of $b+M$, while the R^{--} channel is that of $b-M$, where b and M are scattering lengths for nuclear and magnetic scattering, respectively; and (iii) the matched Pd and Fe layers thicknesses eliminates the *chemical* scattering at the even-order Fourier peaks (Fig. 1),[19] thereby greatly enhancing sensitivity to magnetic scattering from the Pd layers, especially in the R^{--} channel where the peaks are weak at RT due to accidentally matched contrast between Fe (i.e., $b_{Fe}-M$) and Pd (i.e., b_{Pd}).

Visual inspection of Fig. 6 directly leads to the conclusion that Pd is nonuniformly and significantly polarized at 4.5 K. The R^{++} channel at RT [Fig. 6(a)] shows dominant odd-order peaks as the second- and fourth-order peaks are suppressed by the Pd/Fe layer matching. Further suppression due to Fe/Pd contrast matching makes even the odd-order peaks weaker in the R^{--} channel [Fig. 6(b)]. Cooling to 4.5 K leads to a significant increase in intensity at the second-

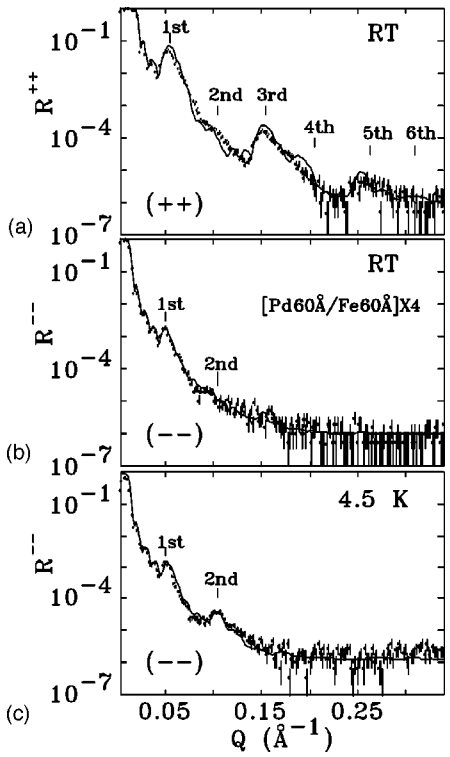

FIG. 6. Polarized neutron reflectometry data at RT and 4.5 K for $[\mathrm{Pd60\ Å/Fe\ 60\ Å}]_4$. Top: the R^{++} channel at RT is dominated by the chemical structure and shows strong odd-order peaks to fifth order. Middle: R^{--} channel at RT showing only the first-order peak. Bottom: R^{--} channel at 4.5 K showing the growth of the second-order peak associated with polarization in the Pd layer. The large change in the second-order R^{--} channel scattering reflects the strong temperature dependence of the Pd polarization. Solid lines are fits as described in the text.

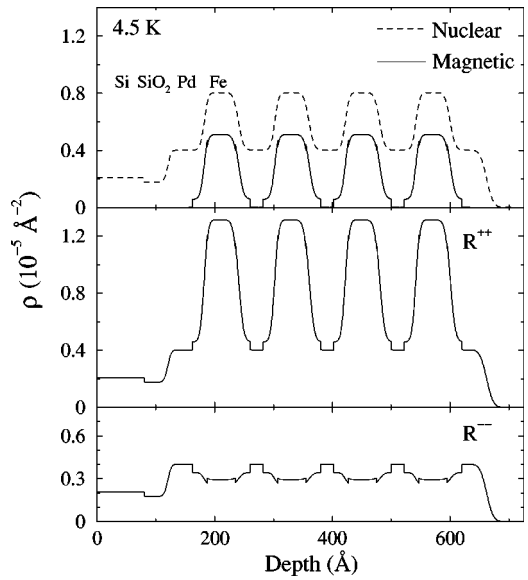

FIG. 7. Top: Magnetic (ρ_M) and nuclear (ρ_n) scattering densities for $[\mathrm{Pd\ 60\ Å/Fe\ 60\ Å}]_4$ at 4.5 K. Middle: The R^{++} channel equals $\rho_M+\rho_n$ and is dominated by the strong correlation between the nuclear and magnetic scattering from the Fe layers. Bottom: The R^{--} channel equals $\rho_M-\rho_n$ and as the two Fe contributions nearly cancel, the large-scale structural contrast is lost, and the R^{--} channel is dominated by the effects of nonuniform moment distributions. Both the enhanced Fe moment at the Pd/Fe interfaces, and the Pd polarization are most clearly seen in the calculated R^{--} profile.

order peak position [Fig. 6(c)], which must be magnetic in origin as the chemical structure cannot change on cooling. Furthermore, the change must be associated with polarization of the Pd layers, since the magnetization of the Fe layers is not strongly temperature dependent (Fig. 5). Increase of intensity at the second-order peak signals deviations from a simple square-wave scattering length profile, and this can only arise in the current system through a significant and nonuniform magnetic polarization of the Pd layers, or a change in the moments of the interfacial Fe. Nonuniformity is an essential feature, as a uniform change within any layer (either Pd, Fe, or both) would simply lead to a change in contrast that would affect *all* Fourier peaks.

In order to provide a quantitative description of the magnetization profile within the Pd/Fe multilayers, we calculate the scattering signals using a matrix method[24] based on classical optical formalism. The analysis code was developed from one used to analyze the x-ray reflectometry data on the same samples. Spot measurements across the 100 mm diameter samples using x-ray reflectometry showed $\sim$10% average thickness variations which were therefore included in the PNR fits. They lead only to a broadening of the reflectivity features, and have no intensity effects. The PNR scattering profile (Fig. 7) included the Si substrate with its native SiO_2 layer. Allowance was also made for interfacial roughness at each Pd/Fe boundary. The Pd and Fe layer thicknesses and the surface roughness parameters were all fixed at values obtained from x-ray reflectometry, the bulk Fe moment was taken to be $2.2\mu_B$, and the thickness of the interfacial Fe layer was set at its CEMS derived value of 4 Å. The three remaining unknown parameters: the interfacial Fe moment m_{i}, the Pd moment m_{Pd} and the thickness of the polarized Pd layer t_{Pd} were adjusted to fit the observed PNR data.

It was immediately apparent that the 4 Å interfacial Fe component seen by CEMS could not, on its own, account for the intensity of the second-order R^{--} channel scattering using either an enhanced or a reduced moment. The 4.5 K R^{--} channel data are very sensitive to the fitting parameters as the first and third peaks set limits on the square-wave contrast between the Fe and Pd layers, whereas the clear second-order peak demands a strong departure from a simple square-wave scattering structure. The best fit to the data (shown as solid lines in Fig. 6) gives the interfacial Fe moment as $m_{\mathrm{i}}=2.4(1)\mu_B/\mathrm{Fe}$ (consistent with CEMS, but now independent of the assumption that B_{hf} scales with μ_{Fe}), the thickness of the polarized Pd layer (at 4.5 K) as $t_{\mathrm{Pd}}=20(4)$ Å, and an average Pd moment of $m_{\mathrm{Pd}}=0.32(2)\mu_B/\mathrm{Pd}$. Fitting the RT data yields $m_{\mathrm{Pd}}=0.11(4)\mu_B/\mathrm{Pd}$ with a reduced thickness of $t_{\mathrm{Pd}}=10(4)$ Å. These results are fully consistent with the values derived from the magnetic and CEMS measurements presented earlier, which of course guided the analysis of the PNR data.

Enhancement of the moment of interfacial Fe is to be expected given the large moments associated with isolated

Fe impurities in Pd.[10,11] The thickness of the interfacial layer is consistent with recent work on molecular-beam epitaxy (MBE) grown Pd/Fe(100) films,[25] however, our moment is somewhat smaller than their $2.7\mu_B$. Similarly, $0.32(2)\mu_B$/Pd is consistent with values obtained from dilute bulk alloys.[2,4] With only 0.36(1) holes in the Pd *d* band[26] an average Pd moment of $0.32(2)\mu_B$ suggests that the Pd *d* band is almost completely polarized for a significant distance from the Fe layer. Previous PNR work on MBE-grown Au/Pd/Fe/Ag samples was unable to detect any Pd polarization,[28] while more recent work at room temperature, also on MBE grown films,[27] reported that the polarization extended no more than four atomic layers from the Fe interface, rather than over eight as found here at 4.5 K. However, the strong temperature dependence of both the amplitude and extent of the Pd polarization observed here shows that low-temperature data are required if clear results are to be obtained. Even at low temperatures, matching of the Pd and 3*d* layer thicknesses is essential to enhance sensitivity to the Pd polarization signal as the null PNR result on some Pd/Co multilayers shows.[29]

V. CONCLUSIONS

Combining data from magnetization, CEMS, and PNR has allowed us to address an issue of fundamental importance in understanding the behavior of an enhanced paramagnet. There is a substantial and extensive polarization of Pd in contact with an Fe surface. At 4.5 K, 20(4) Å of Pd is polarized with an average moment of $0.32(2)\mu_B$/Pd, indicating that the spin-down band is almost full and that most of the 0.36(1) holes in the Pd *d* band[26] are located in the spin-up band. Both the amplitude and the extent of the Pd polarization are strongly temperature dependent. We also find that the Fe moment at the Pd/Fe interface is enhanced to $2.38(2)\mu_B$/Fe for about two atomic layers.

ACKNOWLEDGMENTS

This work was supported by grants from the Natural Sciences and Engineering Research Council of Canada and Fonds pour la formation de chercheurs et l'aide à la recherche, Québec. D.H.R. and L.C. would like to acknowledge extensive help and hospitality from the Neutron Program for Materials Science at Chalk River.

[1] E.C. Stoner, Proc. R. Soc. London, Ser. A **154**, 656 (1936).
[2] J. Crangle, Philos. Mag. **5**, 335 (1960).
[3] R.M. Bozorth, P.A. Wolff, D.D. Davis, V.B. Compton, and J.H. Wernick, Phys. Rev. **122**, 1157 (1961).
[4] J. Crangle and W.R. Scott, J. Appl. Phys. **36**, 921 (1965).
[5] G.J. Nieuwenhuys, Phys. Lett. **43A**, 301 (1973).
[6] F.W. Constant, Phys. Rev. **36**, 1654 (1930).
[7] A.M. Clogston, B.T. Matthias, M. Peter, H.J. Williams, E. Corenzwit, and R.C. Sherwood, Phys. Rev. **125**, 541 (1962).
[8] P.P. Craig, D.E. Nagle, W.A. Stewart, and R.D. Taylor, Phys. Rev. Lett. **9**, 12 (1962).
[9] G.J. Nieuwenhuys, Adv. Phys. **24**, 515 (1975).
[10] J.W. Cable, E.O. Woollan, and W.C. Koehler, J. Appl. Phys. **34**, 1189 (1963).
[11] G.G. Low and T.M. Holden, Proc. Phys. Soc. London **89**, 119 (1966).
[12] M.F. Collins and G.G. Low, Proc. Phys. Soc. London **86**, 535 (1965).
[13] J.W. Cable, E.O. Woollan, W.C. Koehler, and M.K. Wilkinson, J. Appl. Phys. **33**, 1340 (1962).
[14] T.J. Hicks, G.G. Low, and T.M. Holden, J. Phys. C **1**, 528 (1968).
[15] G.G. Low, Adv. Phys. **18**, 371 (1969).
[16] B.H. Verbeek, G.J. Nieuwenhuys, J.A. Mydosh, C. van Dijk, and B.D. Rainford, Phys. Rev. B **22**, 5426 (1980).
[17] J.C. Ododo, J. Phys. F: Met. Phys. **15**, 941 (1985).
[18] A. Oswald, R. Zeller, and P.H. Dederichs, Phys. Rev. Lett. **56**, 1419 (1986).
[19] C. Montcalm, B.T. Sullivan, H. Piépin, J.A. Dobrowolski, and M. Sutton, Appl. Opt. **33**, 2057 (1994).
[20] L. Cheng, Z. Altounian, D.H. Ryan, and J.O. Ström-Olsen, J. Appl. Phys. **91**, 7188 (2002).
[21] A. Boufelfel, R.M. Emrick, and C.M. Falco, Phys. Rev. B **43**, 13 152 (1991).
[22] N. Hosoito, T. Shinjo, and T. Takada, J. Phys. Soc. Jpn. **50**, 1903 (1981).
[23] M. Li, X.D. Ma, C.B. Peng, J.G. Zhao, L.M. Mei, Y.H. Liu, B.G. Shen, and D.S. Dai, J. Phys.: Condens. Matter **6**, L785 (1994).
[24] M. Born and E. Wolf, *Principles of Optics* (Pergamon, Oxford, 1964); S.J. Blundell and J.A.C. Bland, Phys. Rev. B **46**, 3391 (1992); C.F. Majkrzak, Physica B **221**, 342 (1996).
[25] X. Le Cann, C. Boeglin, B. Carrière, and K. Hricovini, Phys. Rev. B **54**, 373 (1996).
[26] J.J. Vuillemin and M.G. Priestly, Phys. Rev. Lett. **14**, 307 (1965); J.J. Vuillemin, Phys. Rev. **144**, 396 (1966); F.M. Mueller, A.J. Freeman, J.O. Dimmock, and A.M. Furdyna, Phys. Rev. B **1**, 4617 (1970).
[27] J. Vogel, A. Fontaine, V. Cros, F. Petroff, J.-P. Kappler, G. Krill, A. Rogalev, and J. Goulon, Phys. Rev. B **55**, 3663 (1997).
[28] J.A.C. Bland, C. Daboo, B. Heinrich, Z. Celinski, and R.D. Bateson, Phys. Rev. B **51**, 258 (1995).
[29] J.A. Borchers, J.F. Ankers, C.F. Majkzak, B.N. Engel, M.H. Wiedermann, R.A. van Leeuwen, and C.M. Falco, J. Appl. Phys. **75**, 6498 (1994).